

Retrieving chlorophyll content in conifer needles from hyperspectral measurements

Yongqin Zhang, Jing M. Chen, John R. Miller, and Thomas L. Noland

Abstract. Spectrally continuous hyperspectral data can be used to detect subtle features in the leaf optical spectra, which correlate especially well with major leaf pigments such as the leaf chlorophyll content. Extensive field and laboratory measurements were carried out at 10 sites in black spruce (*Picea mariana* (Mill.)) forests near Sudbury, Canada, to collect leaf optical spectra, leaf pigment contents, and leaf biophysical parameters. It was found that black spruce needles sampled from different sites, age classes, and branch orientations demonstrated variability in both optical properties and chlorophyll contents. The variability in needle optical spectra showed a good correlation ($R^2 = 0.63$) between the average visible absorptance and needle chlorophyll content. The leaf optical model PROSPECT was modified to incorporate the edge effects of needles on light transfer through them. Two leaf biophysical parameters, namely needle width and thickness, were introduced into the model to take into account the effects of leaf morphology on chlorophyll content retrieval. With the modifications to PROSPECT, the model can capture the variability of needle optical properties and chlorophyll content from the measurements. The retrieval of needle chlorophyll contents was improved with an accuracy of $R^2 = 0.59$ and root mean squared error of $RMSE = 6.32 \mu\text{g}/\text{cm}^2$ compared with the original PROSPECT model with an accuracy of $R^2 = 0.31$ and $RMSE = 9.51 \mu\text{g}/\text{cm}^2$.

Résumé. Les données hyperspectrales spectralement continues peuvent être utilisées pour détecter des caractéristiques subtiles dans les spectres optiques des feuilles qui sont particulièrement bien corrélées avec les pigments majeurs des feuilles, notamment la teneur en chlorophylle des feuilles. Des mesures extensives sur le terrain et en laboratoire ont été réalisées pour dix sites de forêt d'épinette noire (*Picea mariana* (Mill.)) situés près de Sudbury, au Canada, dans le but d'acquérir des spectres optiques des feuilles, la teneur en pigment des feuilles ainsi que les paramètres biophysiques des feuilles. On a observé que les aiguilles de l'épinette noire échantillonnées pour différents sites, différentes classes d'âge et d'orientations des branches exhibaient une variabilité à la fois au niveau des propriétés optiques et des teneurs en chlorophylle. La variabilité dans les spectres optiques des aiguilles affichait une bonne corrélation ($R^2 = 0.63$) entre l'absorptance moyenne dans le visible et la teneur en chlorophylle des aiguilles. Le modèle optique des feuilles PROSPECT a été modifié pour incorporer les effets de bordure des aiguilles sur le transfert de la lumière à travers celles-ci. Deux paramètres biophysiques des feuilles, la largeur et l'épaisseur des aiguilles, ont été intégrés au modèle afin de tenir compte des effets de la morphologie des feuilles sur l'extraction de la teneur en chlorophylle. Avec les modifications apportées au modèle PROSPECT, le modèle peut déceler la variabilité des propriétés optiques des aiguilles et de la teneur en chlorophylle à partir des mesures. L'extraction des teneurs en chlorophylle des aiguilles a été améliorée avec une précision de $R^2 = 0.59$ et $RMSE = 6,32 \mu\text{g}/\text{cm}^2$, par comparaison avec le modèle PROSPECT original, avec une précision de $R^2 = 0,31$ et $RMSE = 9,51 \mu\text{g}/\text{cm}^2$.

[Traduit par la Rédaction]

Introduction

The physiological state of a plant is governed by its biochemical constituents, of which leaf chlorophyll content is both sensitive to environmental conditions and has a strong influence on leaf optical properties and canopy albedo (Blackburn and Pitman, 1999; Baltzer and Thomas, 2005). Leaf chlorophyll content can provide an accurate, indirect estimate of plant nutrient status (Filella et al., 1995; Moran et al., 2000), quantify gross primary production (Gitelson et al., 2006), and

predict wheat grain protein content (Wang et al., 2004). Changes in leaf chlorophyll content and optical properties may have important implications to climate forcing as well (Thomas, 2005). Total leaf chlorophyll content and the ratio of chlorophyll a to b decrease when vegetation is under stress (Fang et al., 1998). Healthy and stressed vegetation present different reflectance features in the green peak and along the red edge due to changes in pigment levels (Rock et al., 1988; Carter, 1994; Gitelson and Merzlyak, 1996; Belanger et al., 1995). The changes of red-edge position and slope are

Received 3 January 2008. Accepted 26 May 2008. Published on the *Canadian Journal of Remote Sensing* Web site at <http://pubs.nrc-cnrc.gc.ca/cjrs> on 29 August 2008.

Y. Zhang¹ and J.M. Chen. University of Toronto, 100 St. George Street, Room 5047, Toronto, ON M5S 3G3, Canada.

J.R. Miller. York University, 4700 Keele Street, Toronto, ON M3J 1P3, Canada.

T.L. Noland. Ontario Forest Research Institute, 1235 Queen Street East, Sault Ste. Marie, ON P6A 2E5, Canada.

¹Corresponding author (e-mail: zhangy@geog.utoronto.ca).

associated with vegetation stress (Chang and Collins, 1983; Horler et al., 1980; 1983; Vogelmann et al., 1993). Canopy reflectance in the green and far-red regions is also sensitive to variations in chlorophyll concentration and can act as an indicator of vegetation stress (Carter, 1994).

Spectrally continuous hyperspectral data are sufficient to detect subtle absorption features in foliar spectra and to study the correlations of vegetation minor absorption features with biochemical parameters. Empirical relationships between leaf reflectance and chlorophyll content have been widely used to estimate leaf chlorophyll content (Gitelson and Merzlyak, 1997; Gitelson et al., 2003; Datt, 1998; 1999). Such indices can serve as indicators of vegetation stress, senescence, and disease and have been used to predict chlorophyll content from field and laboratory measurements of leaf optical spectra (Peñuelas et al., 1998; Gitelson et al., 1999; Gamon et al., 1997). However, these indices lack temporal and spatial continuity because the empirical methods lack a clear mechanistic basis. Process-based models have been developed based on light interactions with the foliar medium to estimate leaf chlorophyll contents as a nondestructive method. These models consider the underlying physics and complexity of the leaf internal structure and therefore are robust and have the potential to replace the statistically based approaches. Jacquemoud and Ustin (2001) reviewed computer-based leaf optical models. Representative models include the N-flux models of Allen and Richardson (1968) and Yamada and Fujimura (1988), the plate models of Allen et al. (1969; 1970) and Jacquemoud and Baret (1990), ray-tracing models (Allen et al., 1973; Ustin et al., 2001), and stochastic and radiative transfer (RT) models such as LEAFMOD (Ganapol et al., 1998). Of these models, PROSPECT (Jacquemoud and Baret, 1990) is simple but effective for estimating leaf reflectance and transmittance with a limited number of input parameters. The model provides a nondestructive measure of leaf chlorophyll contents from leaf optical spectra (Jacquemoud et al., 1996; Kuusk, 1998). PROSPECT has been widely validated for estimating leaf chlorophyll contents of different deciduous species (Zarco-Tejada et al., 2001; 2005; Demarez et al., 1999; Renzullo et al., 2006). With the consideration of leaf thickness factor in the model, seasonal and canopy-height-related variation in chlorophyll content can also be captured (Zhang et al., 2007). Some recent research indicates that the parameterization of the PROSPECT model is insufficient in terms of spectral resolution, the influence of fluorescence, and recalibration of specific absorption coefficient spectra for chlorophyll (le Maire et al., 2004). Nevertheless, studies on broad leaves showed that good accuracy was achieved in chlorophyll content retrieval.

The PROSPECT model was also applied to derive chlorophyll content of conifer needles (Zarco-Tejada et al., 2004). Needles are narrow and thick, and needle structures with adaxial and abaxial surfaces are neither parallel nor necessarily flat planes. The validity of the model for needles needs investigation because the assumption of infinite plane layers as for broad leaves is violated. With the consideration of the needle morphology as an equivalent flat plate, the accuracy of

estimating chlorophyll content in jack pine needles can be improved, although a significant departure remained in the ability of PROSPECT to quantitatively predict the measured optical properties of the needles as a function of pigment content (Moorthy et al., 2008). Needles of different species have distinct morphologies. Black spruce species is an important species in boreal forest ecosystems. Compared to pine needles, black spruce needles are short and narrow, which presents an additional challenge both for accurate measurements of the optical properties and for model development for biochemical content estimation.

The objective of this paper is to improve upon the process-based leaf model PROSPECT for hyperspectral remote sensing applications. Specifically, we present (i) measurements of the optical properties and chlorophyll content of black spruce needles from different sites stratified by age class and branch orientation, (ii) exploration of the potential bias errors of an existing apparatus for measuring needle optical properties, (iii) radiative transfer theories used for modifying PROSPECT for its application to needles with the consideration of the needle shape, and (iv) improvements in needle chlorophyll inversion using the modified PROSPECT.

Materials and measurements

Study sites and needle sampling

Ten black spruce (*Picea mariana* (Mill.) stands (sites SB1–SB10) were selected near Sudbury, Ontario (46°49'13"N to 47°12'9"N, 81°22'2"W to 81°54'30"W), as study sites (**Figure 1**). These 10 sites are large enough (with a pure stand area of at least 20 m × 40 m) for acquiring canopy structural parameters and hyperspectral remote sensing images. In June, July, and August of 2003 and August of 2004, four intensive field campaigns were conducted for collecting leaf samples for laboratory analysis. At each site, two 50 or 60 m long parallel transects separated by 20 m were set up in the east–west or southeast–northwest direction. Five representative trees within a 20 m × 20 m area were marked at each site, and shoots were sampled from the top of tree crowns using a shotgun for chlorophyll analyses. Ten trees (including the five trees for chlorophyll measurements) at each site were marked to measure the average tree height and diameter at breast height (DBH). Basal area was measured with a CM 2 m prism (Prospectors Earth Sciences, Australia) at plot centre for live trees. Leaf area index (LAI) was measured using TRAC (Tracing Radiation and Architecture of Canopies, 3rd-Wave Engineering, Ottawa, Ont.), LAI-2000 (Plant Canopy Analyzer, Li-COR, Lincoln, Nebr.) instruments and digital hemispherical photography (DHP) techniques as described in Zhang et al. (2008). To include the diversity of needles for optical and biophysical measurements and the subsequent chlorophyll retrieval, one additional medium-sized tree from one mature site was selected for analyzing the variation of needle optical, biophysical, and biochemical parameters with respect to needle age and branch orientation. Shoots were sampled in August

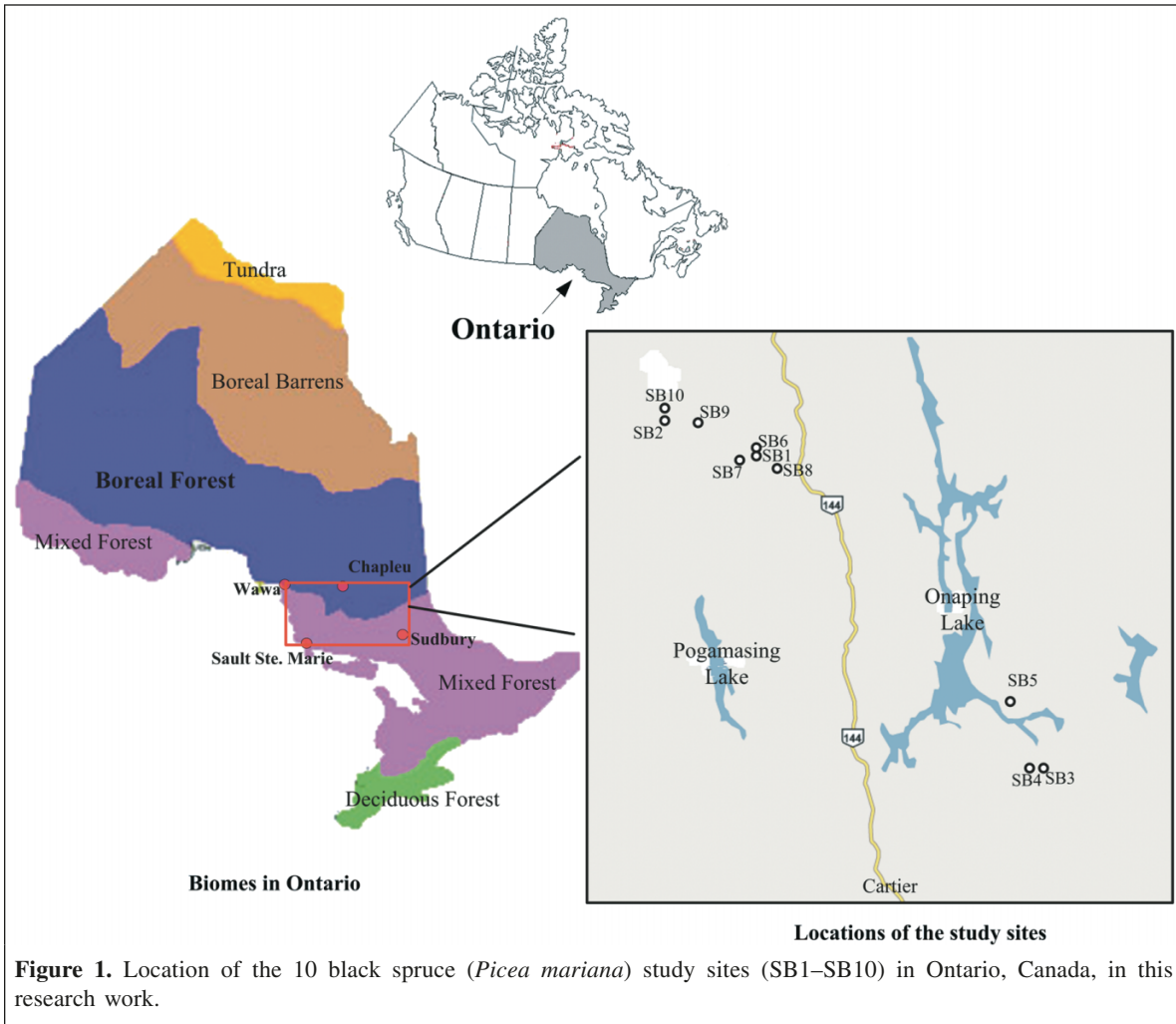


Figure 1. Location of the 10 black spruce (*Picea mariana*) study sites (SB1–SB10) in Ontario, Canada, in this research work.

2004 from four orientations, i.e., north, south, east, and west branches from the tree centre. From each shoot, needles of eight age classes, from the old needles (1998–2003) to the new needles (2004), were taken for the measurements described in the following sections.

Measurements of needle optical properties

Black spruce needles present a challenge for leaf optical spectra measurements due to their small size. As the sample ports of the existing integrating sphere are designed vertically, the key is to present a needle sample to the port of the integrating sphere and avoid any light leakage between the needles within a sample. A spectrometer coupled with an integrating sphere is widely used for the measurements of leaf reflectance and transmittance spectra. We adopted the methodology developed by Harron and Miller (1995) to measure needle optical properties. The measurement protocol effectively eliminates the specular forward scattering effect in the method proposed by Daughtry et al. (1989) and has been evaluated in detail with BOREAS jack pine data (Harron, 2000). A full-range spectroradiometer FieldSpec Pro FR (Analytical Spectral Devices, Inc., Boulder, Colo.) was coupled

with the Li-COR 1800-12S (Li-COR, Inc.) integrating sphere via an optical fibre to measure needle reflectance and transmittance (**Figure 2a**). A pair of specially designed black anodized carriers was used to hold five needles vertically against the sample port of the integrating sphere (**Figure 2b**). With multiple configuration of the light source and various plugs, needle reflectance and transmittance can be measured and derived after quantitatively compensating for the spectral effects of the carrier itself (Harron, 2000). The average adaxial reflectance and transmittance of five needles were measured from 350 to 2500 nm at a 1 nm interval. The new and old needles from the same shoot were measured separately.

Measurements of needle biophysical properties and chlorophyll contents

Following the needle optical measurements, the width and thickness of individual needles were measured using a digital caliper (Marathon Company, Canada). The needles were then stored in separate freezer bags and placed in a cooler with ice (0 °C) for transport to a laboratory and stored at –23 °C after arrival. Further measurements were conducted in a laboratory of the Ontario Forest Research Institute before the needles were

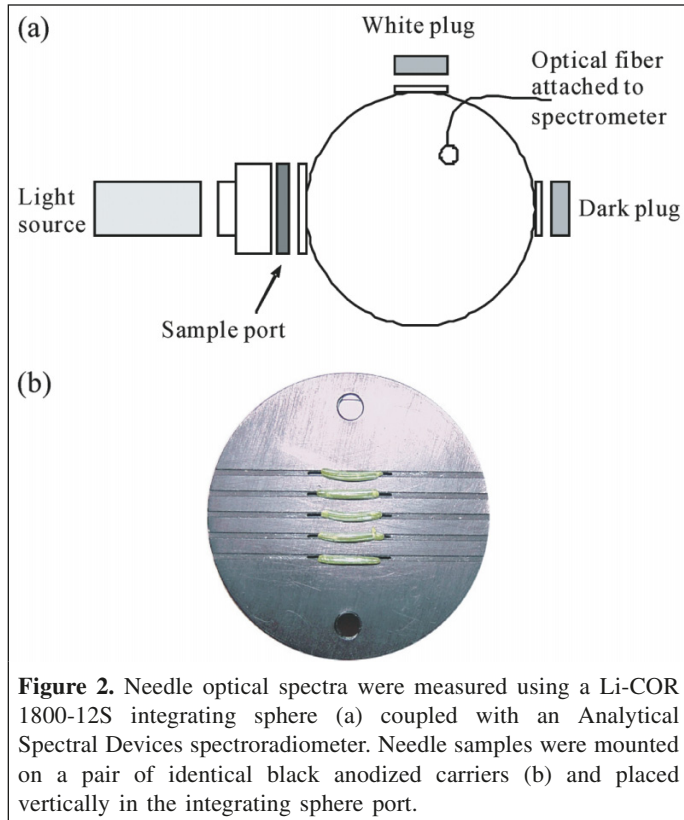


Figure 2. Needle optical spectra were measured using a Li-COR 1800-12S integrating sphere (a) coupled with an Analytical Spectral Devices spectroradiometer. Needle samples were mounted on a pair of identical black anodized carriers (b) and placed vertically in the integrating sphere port.

dehydrated and shrunk. Needle chlorophyll content was measured using the methodology described in Zarco-Tejada et al. (2004) and Moorthy et al. (2008).

Leaf chlorophyll content estimation

Model description

The PROSPECT model is based on the foundational work of Allen and Richardson (1968) and was originally developed for a single compact leaf layer and later extended to multiple layers or plates (Allen et al., 1969; 1970; Gausman et al., 1970). A leaf is assumed to be a stack of N identically thin elementary layers separated by $N - 1$ air spaces. The characteristics of the layers are defined by their refractive index (n) and specific absorption coefficients K_i . The refractive index describes the scattering properties of leaf materials, and N characterizes the leaf mesophyll structure. The elementary layers can absorb light and give rise to scattering of light with their rough surfaces. The overall absorption $K(\lambda)$ is the linear summation of the contents of the biochemicals and the corresponding specific absorption coefficients:

$$K(\lambda) = K_c(\lambda) + \sum K_i(\lambda)C_i / N \quad (1)$$

where λ is the wavelength; $K_c(\lambda)$ is the absorption coefficient of elementary albino and dry matter; C_i is the content of layer constituent i (chlorophyll a and b (chl_{a+b}), liquid water, and dry matter) per unit area; $K_i(\lambda)$ is the corresponding specific

absorption coefficient of constituent i ; and N is the leaf structure parameter, which is the number of compact layers specifying the average number of air – cell walls interfaces within the mesophyll. The model relates leaf biochemistry and scattering parameters to leaf optical signatures using four parameters as inputs. It has been numerically iterated to estimate chlorophyll content by minimizing the following expression:

$$\Delta = \sum_{\lambda} \{ [R_{\text{mes}}(\lambda) - R(\lambda)]^2 + [T_{\text{mes}}(\lambda) - T(\lambda)]^2 \} \quad (2)$$

where R and T are the reflectance and transmittance, respectively, estimated from the model; and R_{mes} and T_{mes} are the leaf reflectance and transmittance, respectively, from measurements.

Model modifications

Accurate measurements of needle optical properties are equally critical to model assessment and development and needle biochemical contents retrieval through model inversion. A series of laboratory experiments was carried out to explore whether there is bias in the measured needle spectra. Modifications were then made to the model based on the experiments and radiative transfer theories.

Effects of needle morphology on leaf optical properties

Laboratory experiments were first conducted to investigate the edge effects of leaf morphology on leaf optical measurements. Twelve less succulent (to minimize the influence and the potential contamination of the internal fluid seeping from the edge of leaf strips) broadleaf species with different leaf thicknesses ranging from 0.38 to 0.76 mm were collected from a greenhouse at the University of Toronto, Toronto. Large leaves were exposed to the sample port of the integrating sphere for measuring reflectance and transmittance. Subsequently, five narrow strips 6.89 mm in length and 1.55 mm in width were cut out from the same area (to simulate needles) and mounted on the needle holding device to measure the “needle” reflectance and transmittance. Apparent differences were found between the spectra of the leaf and leaf strips (needles) cut from the same leaf. **Figures 3a–3d** show the optical characteristics of two *Philodendron cannifolium* (Dryand.) G. Don leaves with thicknesses of 0.38 and 0.51 mm. From the visible to near-infrared regions, the broadleaf demonstrated higher reflectance than leaf-strip reflectance, with large differences in the near-infrared regions (**Figures 3a, 3c**). The discrepancy between leaf and leaf strip is 1.8%–8.3% in the visible reflectance (450–700 nm) and 3.1%–8.6% in the near-infrared reflectance (750–900 nm). A similar trend was found in the transmittance spectra. Little discrepancy was found between leaf and leaf-strip transmittance in the blue and red regions, whereas the discrepancy was evident in the green and near-infrared regions, with maximum discrepancies of 2.2% (**Figure 3b**) and 1.3% (**Figure 3d**) in the green region and

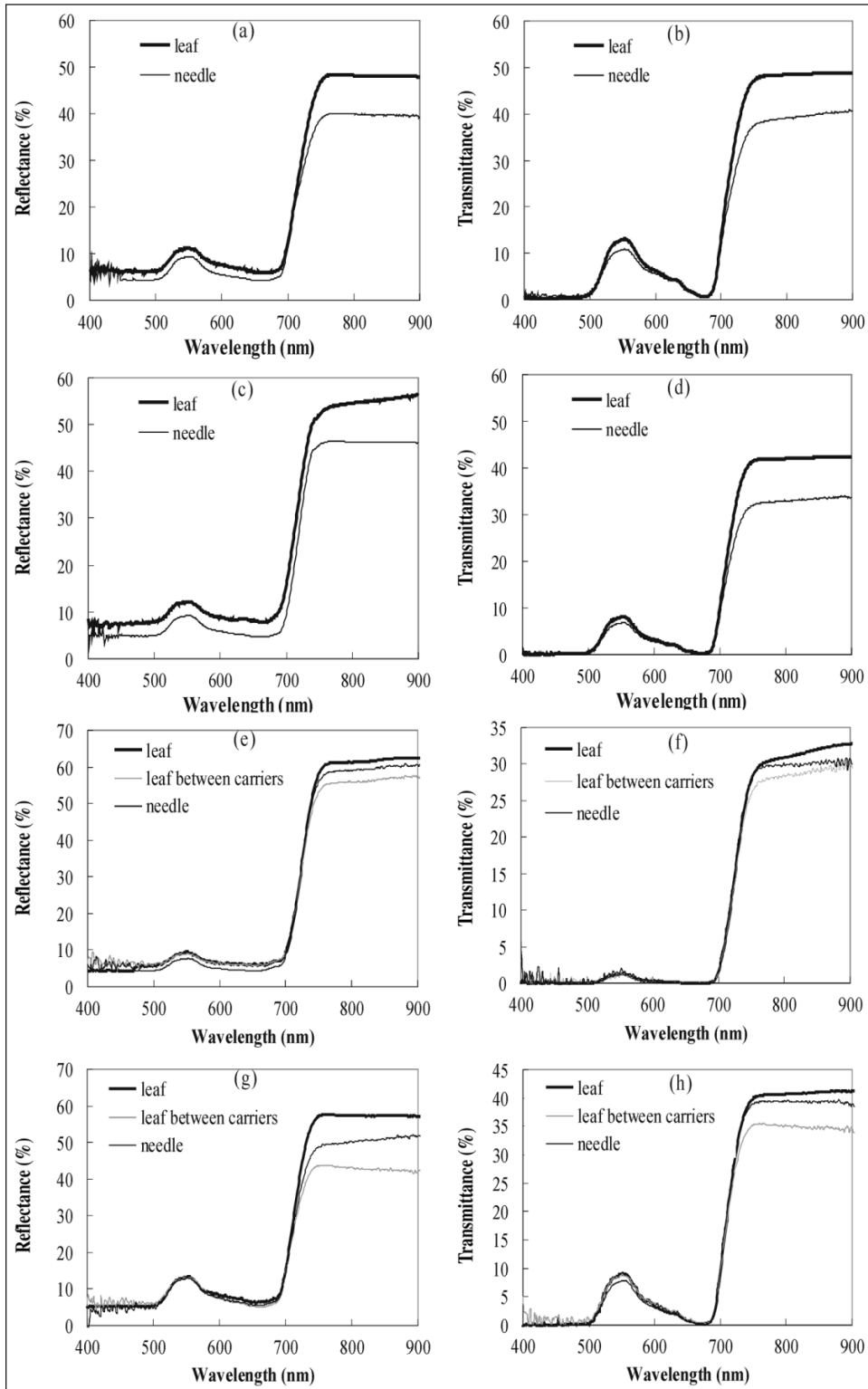


Figure 3. Optical properties of a leaf, a leaf disc clipped between carriers, and leaf strips (needle) cut from the leaf disc: (a, b) reflectance and transmittance spectra of a leaf and needles with thickness of 0.38 mm; (c, d) reflectance and transmittance spectra of a leaf and needles with thickness of 0.51 mm; (e, f) reflectance and transmittance spectra of a leaf, a leaf disc clipped between carriers, and leaf strips (needles) with thickness of 0.33 mm; (g, h) reflectance and transmittance spectra of a leaf, a leaf disc clipped between carriers, and leaf strips (needles) with thickness of 0.48 mm.

9.8% (**Figure 3b**) and 9.4% (**Figure 3d**) in the near-infrared region. Leaf and needle chlorophyll content were estimated with the measured reflectance and transmittance as inputs to the PROSPECT model. For the two leaves shown in **Figures 3a–3d**, the chlorophyll contents of broad leaves are estimated to be 84.8% and 78.1% of those of the corresponding leaf strips.

The experiments also demonstrate the edge effect on leaf spectral measurements as a function of needle thickness. The increasing edge effect on leaf reflectance and transmittance with the leaf thickness is mainly because the number of equivalent horizontal layers in a leaf increases with an increase in leaf thickness (Zhang et al., 2007; Demarez et al., 1999). This implies that light scattering, and therefore the path length of light through the leaf, also increases with an increase in leaf thickness. The detour effect increases absorption and is most pronounced at wavelengths that are weakly absorbed (Vogelmann, 1993). As seen in the transmittance spectra, differences are evident in the green and near-infrared regions (**Figures 3b, 3d**). The reflectance spectrum demonstrated different spectral features from the transmittance in the visible range because the characteristics of reflected light also depend on its origin. Light that is reflected from the cuticle–air interface usually does not vary spectrally, whereas the spectral composition of light originating from the interior of the leaf is strongly influenced by the absorption characteristics of the leaf pigments. Of the reflectance signals, 4.5% of the light is reflected from the adaxial (upper) surface due to the air–cuticle interface, and up to 13% is reflected from the abaxial (lower) leaf surface due to the interior interface and the mesophyll boundary (Vogelmann, 1993). At larger leaf thicknesses, the discrepancy between leaf and needle reflectance is more evident in the pigment absorption region (**Figures 3a, 3c**).

Cutting broad leaves into strips (needles) can cause damage to the leaf tissues, variability between replicate measurements, and problems in signal interpretation. Nevertheless, the effects induced by the leaf morphology and size are undoubtedly evident in leaf optical properties.

Effects of needle-holding device on leaf optical properties

Further experiments were carried out to investigate whether the discrepancy between the spectra of broadleaf and needle was introduced by leaf morphology or the needle-holding apparatus. Measurements on leaves of different thickness followed three procedures. For each whole leaf, the reflectance and transmittance were measured first without the carriers. Then a leaf disc of exactly the same size as the carriers was cut from the same area that was exposed to the sampling port. The leaf disc was clipped between two carriers to acquire the reflectance and transmittance. In this way, the needle carriers expose only the five strips of the leaf disc, approximately representing needle optical spectra measurements. Consequently, the same five leaf strips (needles) were cut from the centre of the leaf disc for needle reflectance and transmittance measurements.

Figures 3e–3h show the experimental results for *Ficus elastica* (Decora) and *Ficus elastica* (Moraceae) leaves with

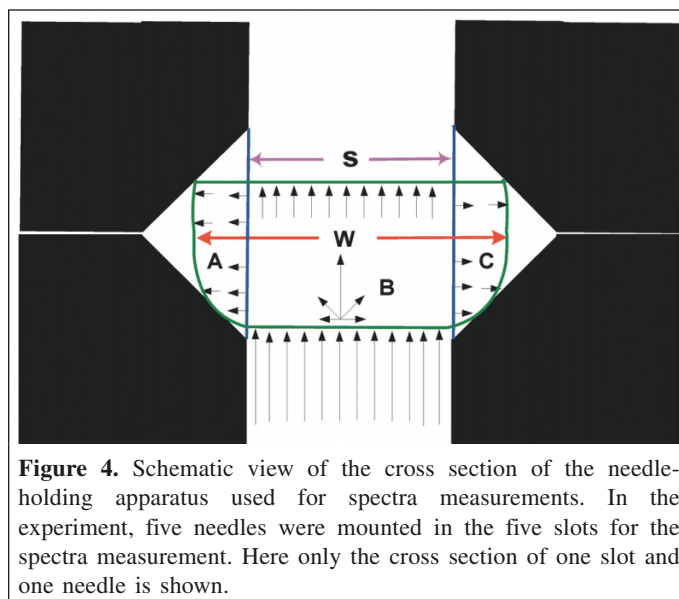


Figure 4. Schematic view of the cross section of the needle-holding apparatus used for spectra measurements. In the experiment, five needles were mounted in the five slots for the spectra measurement. Here only the cross section of one slot and one needle is shown.

thicknesses of 0.33 and 0.48 mm, respectively. Consistent patterns are found in the spectra of a whole leaf, the leaf disc limited in view by needle carriers (denoted as “leaf between carriers” in the figures), and leaf strips (needles) from the same leaf. The discrepancy between the leaf and needle spectra, though small, demonstrated trends similar to those shown in the previous section through the visible to near-infrared regions. In the visible range, little differences were found in reflectance and transmittance spectra between the leaf and the partially exposed leaf disc, suggesting that the discrepancy in the visible region between the leaf and needle spectra is mainly due to the edge effects of needles. Apparent differences were found in the near-infrared region between the leaf, leaf disc with limited view, and needle spectra. For the same leaf species, the spectra of a whole leaf and the same leaf disc with limited view demonstrated significant discrepancy from the red-edge shoulder to the near-infrared region. The geometrical design of carriers causes an underestimation of needle reflectance and transmittance in comparison to those of the same leaf. Of the two cases, the broadleaf demonstrated the highest reflectance and transmittance. The leaf disc clipped between needle carriers showed the lowest reflectance and transmittance. Leaf strips (needles) are the intermediate case. The obstruction effects by the carriers tend to increase with an increase in leaf thickness. For the leaf sample with a thickness of 0.33 mm, the measured average reflectance and transmittance of the leaf disc in the near-infrared region (750–900 nm) are, respectively, 93.1% and 91.5% of those of the same leaf without any obstruction. The effects of needle carriers are more pronounced for the leaf with a thickness of 0.48 mm. The average reflectance and transmittance of the leaf disc are 75.4% and 85.9% of the reflectance and transmittance, respectively, of the same leaf.

Figure 4 schematically illustrates the magnified cross section of one slot of the carrier with one needle. There might be some tiny gaps between the edge of the leaf strip and the

carrier. Light that transfers through the edge of leaf strips might have gone through the gaps, which may have resulted in higher reflectance and transmittance of leaf strips than the leaf disc between the carriers. Along the width direction of the needle, the carrier blocks the two edges of the needle surface, i.e., the curved surface of parts A and C. Only the needle surface in part B is fully exposed to the incoming light. The effective width that light can be transmitted through is the width of the slots (s). The remainder of the incident light is diverged in regions A and C. The width of the carrier slots (s) is 0.8382 mm. Relative to the measurements on the width (w) of black spruce needles, only 38%–70% of the needle surface is exposed to the opening of the slots. The small opening of the slots avoids the light leakage at the leaf edges. However, this creates light divergence within the needles in the lateral directions, which are not captured by the integrating sphere. This lateral light divergence can cause negative biases in the measured needle spectra. The discrepancy due to the obstruction of carriers results in biased estimation of chlorophyll content as well. In the near-infrared region, the measured needle reflectance and transmittance spectra are between those of the whole leaf and those of the partially exposed leaf disc. For the two leaves in **Figures 3e–3h**, the chlorophyll content of the partially exposed leaf disc was estimated to be 98.4% and 94.3%, respectively, of those of the corresponding broadleaf. Due to the low absorption in the near-infrared region, the influence of needle carriers on the chlorophyll retrieval is not significant compared to that of the needle edge effects in the visible region, i.e., leaf morphology plays a main role in the chlorophyll estimation.

We note that the effect of the needle carrier on needle spectral measurements is generally within the two broadleaf measurements with and without the carrier, and the bias errors for the needles appear to be variable between different measurement cases. The variability may result from several factors such as the difference in leaf species and leaf internal structure. For needles of small sizes, consistency in the placement of five needles in the slots of the carriers can also influence the accuracy of spectral measurements.

Model modifications

The interaction of electromagnetic radiation with leaves depends on leaf biochemical and biophysical characteristics. The experiments clearly demonstrate that the PROSPECT model, as designed for broadleaf species, cannot accurately represent the link between the optical properties and the pigment content of needles. Accordingly, we chose to make modifications to the PROSPECT model to take into account the morphological effects of leaf size on the estimation of reflectance and transmittance.

PROSPECT assumes that a leaf is horizontally infinite. The light is either absorbed or transferred upward and downward through the outer layers of a leaf. The assumption may not hold for black spruce needles because the needle thickness is comparable to needle width. Leaf thickness is a factor that influences the light transfer and leaf biochemical content retrieval (Zhang et al., 2007; Slaton et al., 2001). **Figure 5**

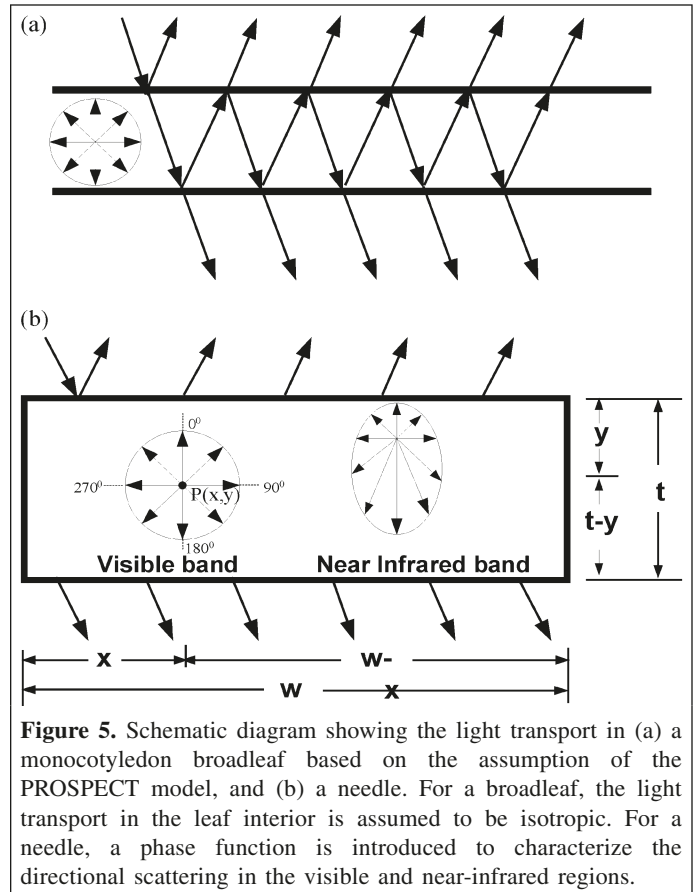


Figure 5. Schematic diagram showing the light transport in (a) a monocotyledon broadleaf based on the assumption of the PROSPECT model, and (b) a needle. For a broadleaf, the light transport in the leaf interior is assumed to be isotropic. For a needle, a phase function is introduced to characterize the directional scattering in the visible and near-infrared regions.

schematically shows the difference between the structural effects of a broadleaf and a needle on light transfer. **Figure 5a** illustrates the light transfer in a broadleaf with a single plate. For leaves with a complex structure, a stack of N macrohomogeneous plates is assumed to account for more complex scattering. As the thickness of a broadleaf is much smaller than the leaf width, the incident light leaves the outer layers as reflected or transmitted light after multiple interactions with the internal plates. Light transmitted through leaf edges is negligible compared with the amount that exits the first (uppermost) and last (lowermost) layers. For thick and narrow black spruce needles (**Figure 5b**), needle length can be assumed to be infinite relative to the leaf thickness and width, but leaf width can significantly affect the measurements of leaf reflectance and transmittance. The needle width is only around two times the leaf thickness. Therefore the amount of light that escapes from needle edges, i.e., along the direction of leaf width, could be large. This portion of light “loss” is not included in the PROSPECT model for the estimation of reflectance and transmittance.

The PROSPECT model considers that the incoming light is incident within a solid angle. After the light penetrates inside the leaf, the light scattering is assumed to be isotropic in all directions. For black spruce needles, we assume light is scattered towards the leaf thickness and width direction unevenly. A phase function was introduced to describe the directional scattering from the incoming direction to the

outgoing direction of the light. As particles contained in a leaf interior are of different sizes, simple single-particle phase functions are not applicable. The Henyey–Greenstein phase function is often used to characterize the angular distribution of scattered light in layered materials such as biological tissues of leaves (Hanrahan and Krueger, 1993). The phase function is as follows (Henyey and Greenstein, 1941):

$$p(\cos \theta) = \frac{1-g^2}{4(1+g^2-2g \cos \theta)^{3/2}} \frac{1}{4\pi} \quad (3)$$

where θ is the angle between the incoming and outgoing directions, and g is the average cosine of the scattered angle. The Henyey–Greenstein phase function is characterized by the parameter g . Light scattering is symmetric about the incident direction. For different values of g , the Henyey–Greenstein phase function indicates different scattering as follows:

$$\begin{cases} g = 0: \text{isotropic scattering} \\ g > 0: \text{predominantly forward scattering} \\ g < 0: \text{predominantly backward scattering} \end{cases}$$

Shorter wavelengths of light are preferentially scattered in comparison to longer wavelengths (DeLucia et al., 1992). In the near-infrared region where the absorption of light is low, the internal structure of a leaf controls reflectance and transmittance. Based on our experimental results as shown in **Figure 3**, we assume that the light scattering is spectrally different in the visible and near-infrared ranges, i.e., different g values are required for describing the scattering process across the visible and near-infrared regions. The value of g can be determined through an optimization procedure. When the incoming light penetrates through the upper leaf surface, it is scattered at $P(x, y)$ (**Figure 5b**). We denote the leaf width as w ; the leaf thickness as t ; and the light scattered towards the leaf width (along 90° and 270°) and thickness (along 0° and 180°) directions as $L_{\text{width}}(w)$ and $L_{\text{thick}}(t)$, respectively. A_g is the global absorption coefficient by chl_{a+b}, liquid water, and biochemicals. Based on Beer’s law, $L_{\text{width}}(w)$ and $L_{\text{thick}}(t)$ can be calculated as follows:

$$L_{\text{width}}(x) = \exp[-A_g P(\cos 90^\circ)x] + \exp[-A_g P(\cos 270^\circ)(w-x)] \quad (4)$$

$$L_{\text{thick}}(y) = \exp[-A_g P(\cos 0^\circ)y] + \exp[-A_g P(\cos 180^\circ)(t-y)] \quad (5)$$

The total light penetrating through the leaf width and thickness are then given as follows:

$$L_{\text{width}} = \frac{1}{w} \int_0^w \{ \exp[-A_g P(\cos 90^\circ)x] + \exp[-A_g P(\cos 270^\circ)(w-x)] \} dx \quad (6)$$

$$L_{\text{thick}} = \frac{1}{t} \int_0^t \{ \exp[-A_g P(\cos 0^\circ)y] + \exp[-A_g P(\cos 180^\circ)(t-y)] \} dy \quad (7)$$

These two portions of light are not accounted for in the simulation of leaf reflectance and transmittance by PROSPECT. With the consideration of these two portions of light transfer, the corresponding reflectance R_{width} and transmittance T_{width} losses from the needle width direction can be simply inferred from the following measurements:

$$R_{\text{width}} = \frac{L_{\text{width}}}{\frac{1}{t} \int_0^t \exp[-A_g P(\cos 0^\circ)y] dy} R_{\text{mes}} \quad (8)$$

$$T_{\text{width}} = \frac{L_{\text{thick}}}{\frac{1}{t} \int_0^t \exp[-A_g P(\cos 180^\circ)y] dy} T_{\text{mes}} \quad (9)$$

Then the following adjustments were given to estimate needle reflectance and transmittance:

$$R_{\text{mod}} = R - R_{\text{width}} \quad (10)$$

$$T_{\text{mod}} = T - T_{\text{width}} \quad (11)$$

where R_{mod} and T_{mod} are the needle reflectance and transmittance, respectively, after modifications; and R and T are the reflectance and transmittance, respectively, estimated from the PROSPECT model.

Chlorophyll estimation

Needle optical properties and chlorophyll content were estimated using both the modified and original PROSPECT models as a comparison. Due to the low intensity of the halogen lamp in the ultraviolet and short-wave infrared regions, only the spectra values from 400 to 950 nm were used. PROSPECT requires four input parameters to simulate leaf reflectance and transmittance. However, from 400 to 800 nm, only chl_{a+b} content and the structural parameter N contribute to the variation in leaf optical properties in the PROSPECT model. With the measured chl_{a+b} content and N obtained from the PROSPECT inversion model through mathematical iteration as inputs, needle reflectance and transmittance spectra can be estimated. Chlorophyll content was retrieved from measured needle reflectance and transmittance. For the modified PROSPECT model, half of the needle samples were first input to the model to determine the optimal g values for the visible and near-infrared regions. Chlorophyll contents were then estimated with the g values applied for all the samples. The root mean square error (RMSE) was calculated to estimate the deviation between the estimated and measured chlorophyll content.

Table 1. Black spruce (*Picea mariana* (Mill.)) site characteristics.

Site	Lat. (°N)	Long. (°W)	Estimated age (years) ^a	Tree height (m)	Basal area (m ² /ha) ^b	DBH (cm)	Leaf area index, LAI	Condition
SB1	47.164	81.742	115	13.89±1.63	15	15.44±1.38	3.30	Healthy
SB2	47.202	81.908	95	15.72±1.12	10	19.60±1.75	3.97	Healthy
SB3	46.821	81.368	75	14.08±0.73	12	16.38±1.97	2.36	Stressed
SB4	46.820	81.375	120	17.78±2.37	24	18.28±3.39	3.21	Stressed
SB5	46.907	81.420	100	12.58±2.31	17	12.14±1.88	3.09	Healthy
SB6	47.164	81.743	155	17.10±1.47	27	14.78±2.77	3.78	Healthy
SB7	47.163	81.746	35	4.90±2.02	3	5.58±2.89	1.14	Stressed
SB8	47.162	81.727	40	6.56±3.03	9	6.58±2.73	2.88	Stressed
SB9	47.199	81.867	45	11.20±0.83	17	10.22±1.15	3.83	Healthy
SB10	47.203	81.908	85	13.28±2.46	15	15.08±4.01	5.37	Healthy

^aBased on look-up tables of site index curves found in Plonski (1974).

^bCross-sectional area of the tree trunks per hectare (as a measure of tree density).

Results

The 10 black spruces sites are of different ages, tree heights and sizes, stand densities, health conditions, and canopy closures (**Table 1**). Needles from different sites, age classes, and branch orientations show a large variability and dynamic range in optical properties and chlorophyll contents.

Needle optical properties

The weighted (old and new needles) average reflectance spectra of the 10 sites showed small differences in the blue region, and larger differences were found from the green to near-infrared regions, ranging from $18.0 \pm 2.9\%$ to $27.8 \pm 2.2\%$ at 550 nm, $7.8 \pm 2.3\%$ to $12.1 \pm 0.7\%$ at 670 nm, and $39.0 \pm 4.9\%$ to $45.8 \pm 2.3\%$ at 800 nm. The differences in the weighted average transmittance spectra among the 10 sites were small in the blue and red regions. In the green and near-infrared regions, the 10 transmittance spectra varied from $1.9 \pm 0.6\%$ to $5.2 \pm 4.1\%$ and from $21.7 \pm 3.7\%$ to $29.3 \pm 9.2\%$, respectively.

Needle samples from different branch orientations demonstrated variability in leaf optical properties. Though needle reflectance differed between the north–south and east–west orientations, little difference was found in the reflectance spectra between the east and west branches and between the north and south branches. In the visible region, needle transmittance showed little difference. In comparison, notable differences were observed in the near-infrared region.

Needles of different age classes presented distinct differences in both reflectance and transmittance spectra in the near-infrared region, with old needles showing higher reflectance and transmittance than new needles. Variation in the reflectance and transmittance was observed in the visible region, though there was no obvious trend with respect to age.

Needle chlorophyll content

Individual needle samples provided about a four-fold dynamic range in chlorophyll content for the model test and validation. Needle chlorophyll content varies among the 10 sites, with the average chlorophyll content ranging from

$19.53 \pm 5.89 \mu\text{g}/\text{cm}^2$ (site SB3) to $33.55 \pm 10.99 \mu\text{g}/\text{cm}^2$ (site SB10) (**Figure 6a**). From the same site, the average needle chlorophyll content varied in each sample of five needles. The standard deviation ranged from 4.59 to $10.99 \mu\text{g}/\text{cm}^2$. The reasons for the differences in chlorophyll content between sites are not clear but may be due to different environmental stress factors. Needles from branches of different orientations showed differences in chl_{a+b} content, though they were not significant (**Figure 6b**). The highest and lowest chlorophyll contents were found in the needles from the south and east branches, with 35.18 ± 5.93 and $31.18 \pm 5.88 \mu\text{g}/\text{cm}^2$, respectively. Variations of needle chl_{a+b} content from different age classes were also noticeable (**Figure 6c**). As expected, old needles exhibited higher chlorophyll content than new needles for all sites (**Figure 6d**). The chlorophyll content ranged from 23.20 ± 4.29 to $40.49 \pm 7.80 \mu\text{g}/\text{cm}^2$ for old needles and from 14.01 ± 0.82 to $23.15 \pm 0.39 \mu\text{g}/\text{cm}^2$ for new needles. The average needle chlorophyll content of the age class 1999 was the highest ($37.59 \pm 2.31 \mu\text{g}/\text{cm}^2$), with the next highest being the age class 2001 ($37.48 \pm 5.09 \mu\text{g}/\text{cm}^2$). New needles (age class 2004) showed the lowest average chlorophyll content of $24.06 \pm 3.08 \mu\text{g}/\text{cm}^2$.

Needles with higher absorption spectra throughout the visible region were associated with higher chlorophyll contents (**Figure 7**). The average absorbance ($1 - \text{reflectance} - \text{transmittance}$) in the visible region correlated well with the average chlorophyll content with respect to site, age, and branch orientation ($R^2 = 0.63$). This finding is in agreement with previous research showing that leaf absorption spectra are driven by the chlorophyll content (Thomas and Gausman, 1977; Agustí et al., 1994; Gitelson and Merzlyak, 1994).

Needle chlorophyll content estimation

The PROSPECT model estimated needle chl_{a+b} content of all samples with an accuracy of $R^2 = 0.31$ and RMSE = $9.51 \mu\text{g}/\text{cm}^2$ (**Figure 8**). Needle chlorophyll content tends to be underestimated due to the overestimation of needle reflectance and transmittance.

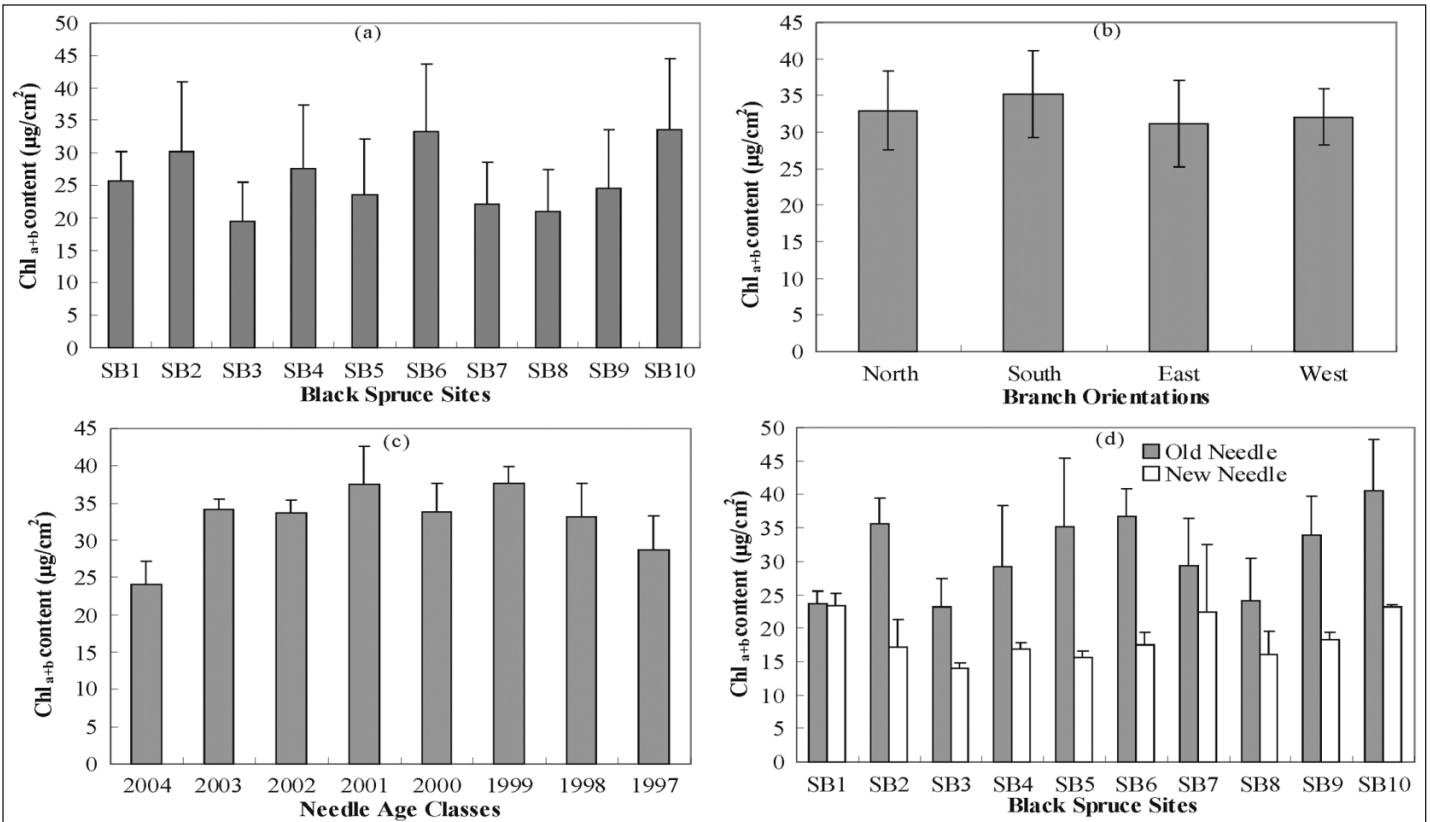


Figure 6. Variation of needle chl_{a+b} content (means and one standard deviation are shown) from the 10 black spruce sites: (a) needle chl_{a+b} content from the 10 black spruce sites; (b) chl_{a+b} content of needle from four different branch orientations, i.e., north, south, east, and west branches; (c) chl_{a+b} content of different needle age classes; (d) chl_{a+b} content of old and new needles.

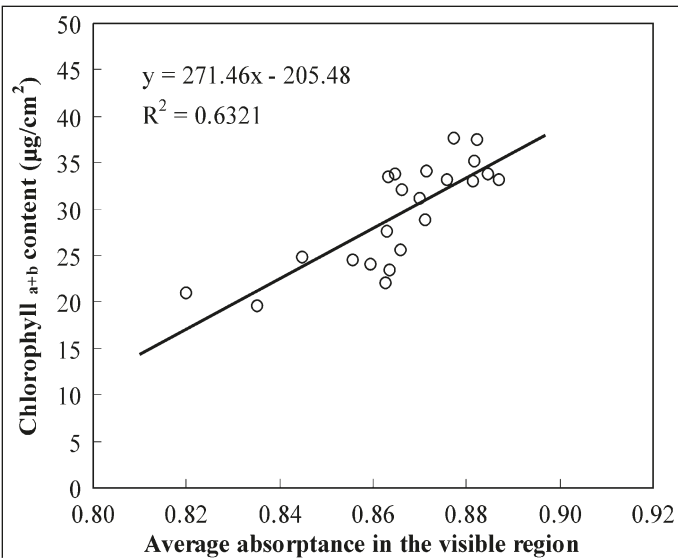


Figure 7. The correlation between the average absorbance in the visible region and the average chlorophyll content.

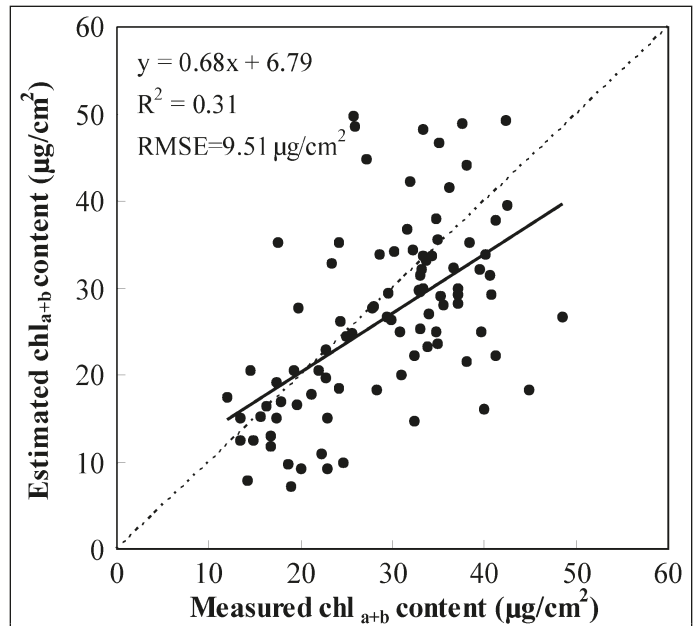


Figure 8. Relationship between the measured and estimated chlorophyll contents using the original PROSPECT inversion model. The broken line is the 1:1 line.

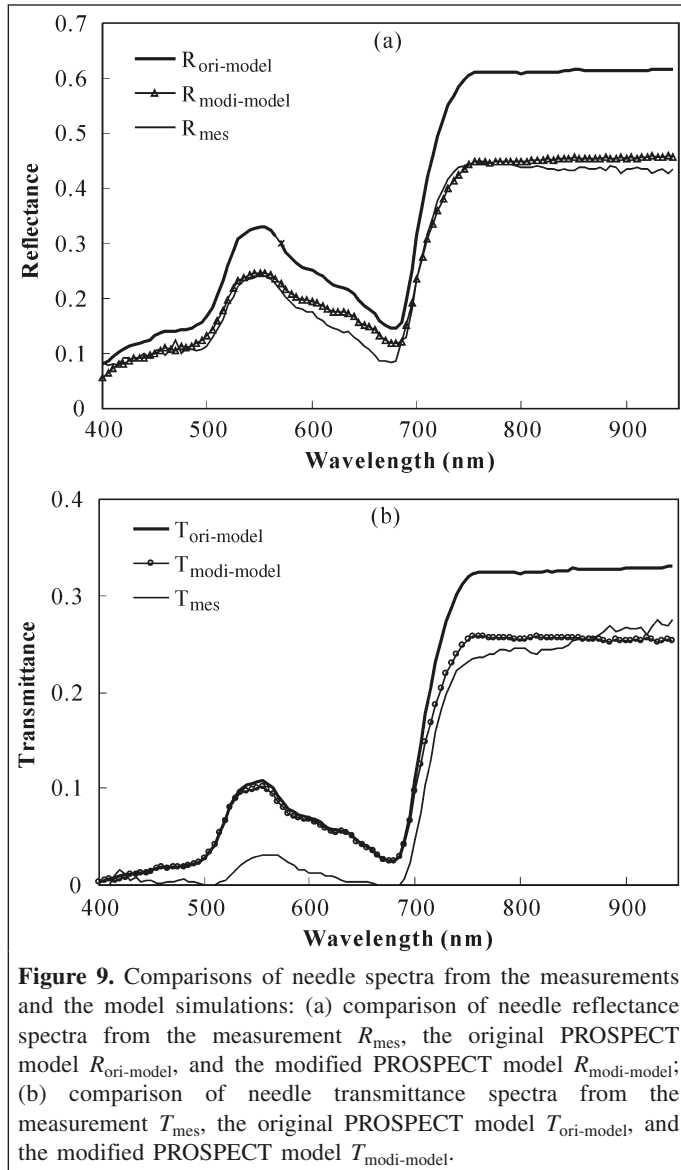


Figure 9. Comparisons of needle spectra from the measurements and the model simulations: (a) comparison of needle reflectance spectra from the measurement R_{mes} , the original PROSPECT model $R_{ori-model}$, and the modified PROSPECT model $R_{modi-model}$; (b) comparison of needle transmittance spectra from the measurement T_{mes} , the original PROSPECT model $T_{ori-model}$, and the modified PROSPECT model $T_{modi-model}$.

Our measurement showed that the average length, thickness, and width of black spruce needles were 7.03 ± 0.82 , 0.91 ± 0.11 , and 1.60 ± 0.26 mm, respectively. The optimum values of g were determined to be 0.0 in the visible region and 0.6 in the near-infrared region, i.e., light is scattered isotropically in the visible region but predominantly in the forward direction in an elongated shape in the near-infrared region, as sketched in **Figure 5b**. Incorporating needle thickness and width in the model improved the estimation of needle reflectance and transmittance, in comparison to the original PROSPECT model, from the visible to near-infrared ranges (**Figure 9**). The overestimation of needle reflectance and transmittance is in accordance with the finding of Dawson et al. (1995). The discrepancy between the estimated and measured spectra was particularly apparent in the near-infrared range, though the degree varied among samples. The average and minimum discrepancies between $R_{ori-mod}$ and R_{mes} were 10.71% and 0.24%, respectively, with a maximum discrepancy of 18.85% at

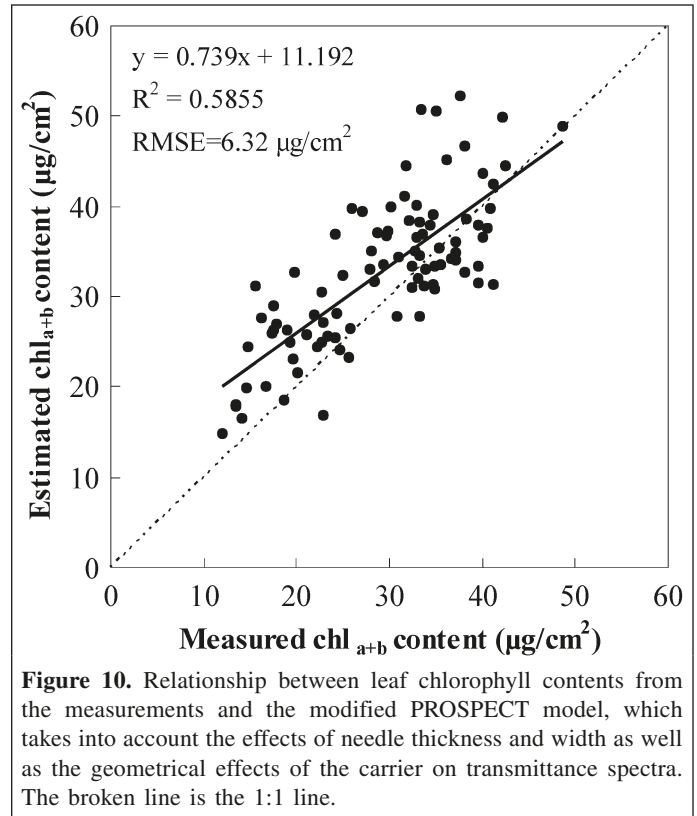


Figure 10. Relationship between leaf chlorophyll contents from the measurements and the modified PROSPECT model, which takes into account the effects of needle thickness and width as well as the geometrical effects of the carrier on transmittance spectra. The broken line is the 1:1 line.

925 nm. With the modifications to the model, the average and minimum discrepancies between reflectance from measurements and from the modified model were 1.61% and 0.04%, respectively, and the maximum discrepancy was 4.68% at 660 nm. The average and minimum discrepancies between $T_{mor-mod}$ and T_{mes} were 5.49% and 0.20%, respectively; in comparison, the average and minimum discrepancies between $T_{modi-mod}$ and T_{mes} were 2.76% and 0.06%, respectively. The maximum difference between the estimated and measured transmittance was reduced from 8.90% at 755 nm to 6.91% at the green peak (550 nm). In particular, the improvement was notable in the near-infrared region. The discrepancy between the modeled and measured spectra was minimized from 7.3% to 1.2%. The improvement for the visible band was not significant. A sensitivity test was given with a range of g values as inputs for the visible range. We found that it is impossible to simulate the measured transmittance spectra in the visible range. This is because the modifications were based on the measurements. The measured transmittance was very low in the visible bands, and this leads to a small modification to the visible transmittance. This also implies the broadleaf model PROSPECT cannot capture the optical features of thick needle leaves.

With the modifications to the model for reflectance and transmittance estimation, the chlorophyll content inversion was improved with $R^2 = 0.59$ and $RMSE = 6.32 \mu\text{g}/\text{cm}^2$ (**Figure 10**). The modified model captures the variation of needle chlorophyll content well from different sites, age classes, and branch orientations. These results showed an improvement on

the chlorophyll estimation results with jack pine needles ($R^2 = 0.54$ and $RMSE = 7.9 \mu\text{g}/\text{cm}^2$) reported by Moorthy et al. (2008), using PROSPECT with a simple compensation for needle shape. As black spruce needles are significantly smaller and more difficult to measure than jack pine needles, the improvements achieved by our new approach are significant.

Sensitivity tests on model parameters

The modified model can be applicable to estimating leaf biochemical contents of other types of conifer needles. For different needles, needle thickness and width may vary, thus the effects on the reflectance and transmittance estimation may differ. **Figure 11** demonstrates the effects of needle width on the estimation of reflectance and transmittance spectra. The figure shows that when the needle width is changed by a factor of 10, 20, and 50 compared with the original needle width while keeping the same thickness, the estimated needle reflectance and transmittance from the modified model approach those from the original PROSPECT model. In the visible region, when needle width is changed to 10 times that of black spruce needles, the simulated reflectance and transmittance agree well with the simulations from the original PROSPECT model, indicating that for these widths the modified model is in conformity with the horizontally infinite assumption of the PROSPECT model. The influences of needle width on the estimation of needle spectra are pronounced in the near-infrared region. At 50 times the original width, the remaining width effect is about zero in the visible range and 2.4% in the near-infrared region for the reflectance measurements.

The sensitivity of the estimated reflectance and transmittance to needle thickness was also explored (**Figure 12**). As leaf thickness is closely related to the structural parameter N in the model, the corresponding change of N in relation to leaf thickness is considered in the sensitivity test (Zhang et al., 2007). Increasing needle thickness gradually by a factor of 1.1 ($1.1t$), 1.2 ($1.2t$), and 1.3 ($1.3t$) results in a gradual increase in the estimated reflectance and a decrease in leaf transmittance. At $1.3t$ (where $N \approx 3$), the estimated reflectance in the visible range approaches those from the original PROSPECT model.

Discussion

This study demonstrates that needle biophysical parameters, namely needle thickness and width, influence the light transfer through needles. Incorporating needle thickness and width in the broadleaf model PROSPECT for the application to needle species improves the estimates of chlorophyll content. These two biophysical parameters are easy to acquire through laboratory measurements, which facilitate the implementation of modeling efforts. However, the one-to-one correspondence in the estimated versus measured total needle chlorophyll content still needs improvement. It is also noted that the measured visible transmittance is much smaller than the estimation from the original and modified models, and the effect of the carriers

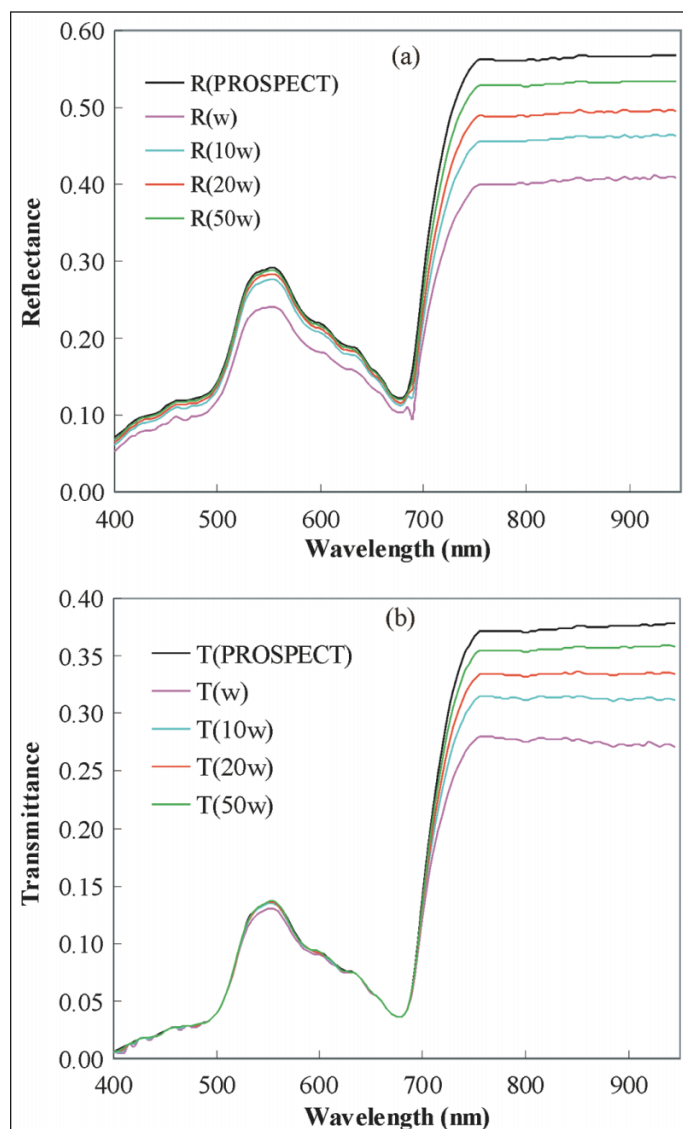
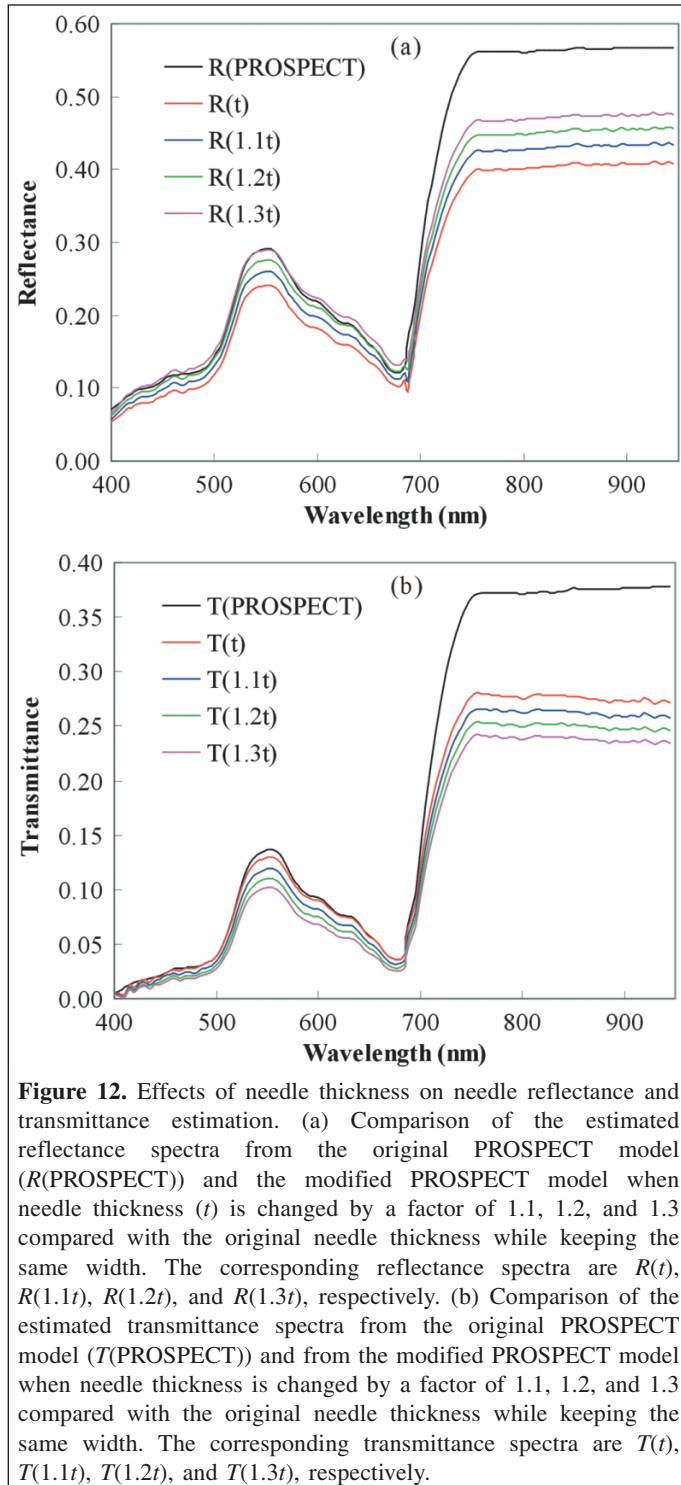


Figure 11. Effects of needle width on needle reflectance and transmittance estimation. (a) Comparison of the estimated reflectance spectra from the original PROSPECT model ($R(\text{PROSPECT})$) and from the modified PROSPECT model when needle width (w) is changed by a factor of 10, 20, and 50 compared with the original needle width while keeping the same thickness. The corresponding reflectance spectra are $R(w)$, $R(10w)$, $R(20w)$, and $R(50w)$, respectively. (b) Comparison of the estimated transmittance spectra from the original PROSPECT model ($T(\text{PROSPECT})$) and from the modified PROSPECT model when needle width (w) is changed by a factor of 10, 20, and 50 compared with the original needle width while keeping the same thickness. The corresponding transmittance spectra are $T(w)$, $T(10w)$, $T(20w)$, and $T(50w)$, respectively.

seems to be small in the visible spectrum. This necessitates further model refinements specific to the needle structure. Development of a completely new process-based, leaf-level spectral model applicable to needle forms is also encouraged.

Accurate measurements of needle spectra are critical for the retrieval of leaf chlorophyll content. This research adopted the available carrier-based methods to measure needle spectra. The



geometrical design of carriers for spectral measurement causes bias errors in the needle reflectance and transmittance, especially in the near-infrared region. The potential effects of the carrier on leaf optical spectra measurements and the resulting chlorophyll content retrieval were investigated. However, the inherent bias in the measured needle spectra due to the device is not eliminated. A new apparatus is desirable for needle spectrum measurement. It can be designed based on the

findings of this study. The key is to minimize the effects of a needle-holding device on the measurements of needle spectra. This new apparatus should be able to hold small needles while still preventing the leakage or loss of light from the edges and exposing the needle surface to the light source as much as possible. Ideally, needles can be fully exposed to the light source across the width, and the slot openings of the carrier are adjustable for needles of variable widths.

Conclusion

This research improved a process-based broadleaf optical model PROSPECT for estimating needle chlorophyll content. Needleleaf species make up the largest biome of boreal forest ecosystems, of which black spruce represents a dominant portion. Methodologies developed for black spruce needles would be particularly useful for remote sensing applications to boreal landscapes. Based on radiative transfer theories, the effects of needle width and thickness on light transfer were incorporated in the model. With the modifications, the model developed for deciduous leaves can be applied with a reasonable accuracy to coniferous needles for the estimation of their biochemical contents. Needle chlorophyll content retrieval from measured optical spectra was improved from $R^2 = 0.31$ and $\text{RMSE} = 9.51 \mu\text{g}/\text{cm}^2$ to $R^2 = 0.59$ and $\text{RMSE} = 6.32 \mu\text{g}/\text{cm}^2$. The needle samples investigated in this research were collected from stands with a good variety of environmental variables. The modified PROSPECT model can be used for needle species with greater confidence than the original model. Nevertheless, this improvement in the applicability of PROSPECT to needles did not appreciably reduce the departure of the slope of the estimated versus measured total needle chlorophyll content from the 1:1 line. This remaining issue calls for further model refinements specific to the needle internal structure. The apparatus used in this study for measuring needle reflectance and transmittance spectra limits the leaf area exposed to the light source and results in a negative bias in the spectra measurements from the red edge to the near-infrared region, and accordingly an underestimation of chlorophyll content. A new apparatus that can fully expose the upper needle surface to the light source is desirable for accurate needle spectral measurements.

Acknowledgments

This research is funded by the GEOIDE project Imaging Spectroscopy: Developments for Renewable and Mineral Resources and a discovery grant from the Natural Sciences and Engineering Research Council of Canada. We gratefully acknowledge Inian Moorthy of York University for instructions on leaf spectral measurements. We also thank Denzil Irving, Maara Packalen, and Lesley Rich of the Ontario Forest Research Institute for leaf sampling and chlorophyll extraction, and Mingzhen Chen and Gang Mo of the University of Toronto for field assistance. Dr. Stephen Jacquemoud kindly provided the PROSPECT source

code and several useful instructions. Four anonymous reviewers gave valuable suggestions on the paper revision.

References

- Agustí, S., Enriquez, S., Frost-Christensen, H., Sand-Jensen, K., and Durate, C.M. 1994. Light harvesting among photosynthetic organisms. *Functional Ecology*, Vol. 8, pp. 273–279.
- Allen, W.A., and Richardson, A.J. 1968. Interaction of light with a plant canopy. *Journal of the Optical Society of America*, Vol. 58, No. 8, pp. 1023–1028.
- Allen, W.A., Gausman, H.W., Richardson, A.J., and Thomas, J.R. 1969. Interaction of isotropic light with a compact plant leaf. *Journal of the Optical Society of America*, Vol. 59, No. 10, pp. 1376–1379.
- Allen, W.A., Gausman, H.W., and Richardson, A.J. 1970. Mean effective optical constants of cotton leaves. *Journal of the Optical Society of America*, Vol. 60, No. 4, pp. 542–547.
- Allen, W.A., Gausman, H.W., and Richardson, A.J. 1973. Willstätter-Stoll theory of leaf reflectance evaluation by ray tracing. *Applied Optics*, Vol. 12, No. 10, pp. 2448–2453.
- Baltzer, J.L., and Thomas, S.C. 2005. Leaf optical responses to light and soil nutrient availability in temperate deciduous trees. *American Journal of Botany*, Vol. 92, pp. 214–223.
- Belanger, M.J., Miller, J.R., and Boyer, M.G. 1995. Comparative relationships between some red edge parameters and seasonal leaf chlorophyll concentrations. *Canadian Journal of Remote Sensing*, Vol. 21, No. 1, pp. 16–21.
- Blackburn, G.A., and Pitman, J.I. 1999. Biophysical controls on the directional spectral reflectance properties of bracken (*Pteridium aquilinum*) canopies: results of a field experiment. *International Journal of Remote Sensing*, Vol. 20, No. 11, pp. 2265–2282.
- Carter, G.A. 1994. Ratios of leaf reflectances in narrow wavebands as indicators of plant stress. *International Journal of Remote Sensing*, Vol. 15, pp. 697–704.
- Chang, S., and Collins, W. 1983. Confirmation of the airborne biogeophysical mineral exploration technique using laboratory methods. *Economic Geology*, Vol. 1983, pp. 723–736.
- Datt, B. 1998. Remote sensing of chlorophyll a, chlorophyll b, chlorophyll a+b, and total carotenoid content in Eucalyptus leaves. *Remote Sensing of Environment*, Vol. 66, pp. 111–121.
- Datt, B. 1999. Visible/near infrared reflectance and chlorophyll content in Eucalyptus leaves. *International Journal of Remote Sensing*, Vol. 20, pp. 2741–2759.
- Daughtry, C.S.T., Biehl, L.L., and Ranson, K.J. 1989. A new technique to measure the spectral properties of conifer needles. *Remote Sensing of Environment*, Vol. 27, pp. 81–91.
- Dawson, T.P., Curran, P.J., and Plummer, S.E. 1995. Modelling the spectral response of coniferous leaf structures for the estimation of biochemical concentrations. In *Remote Sensing in Action(RSS95): Proceedings of the 21st Annual Conference of the Remote Sensing Society*, 11–14 September 1995, Southampton, UK Remote Sensing Society, Nottingham, UK. pp. 587–594.
- DeLucia, E.H., Day, T.A., and Vogelmann, T.C. 1992. Ultraviolet-B and visible light penetration into needles of two species of subalpine conifers during foliar development. *Plant Cell and Environment*, Vol. 15, pp. 921–929.
- Demarez, V., Gastellu-Etchegorry, J.P., Mougou, E., Marty, G., and Proisy, C. 1999. Seasonal variation of leaf chlorophyll content of a temperate forest: inversion of the PROSPECT model. *International Journal of Remote Sensing*, Vol. 20, pp. 879–894.
- Fang, Z., Bouwkamp, J., and Solomos, T. 1998. Chlorophyllase activities and chlorophyll degradation during leaf senescence in nonyellowing mutant and wild type of *Phaseolus vulgaris* L. *Journal of Experimental Botany*, Vol. 49, pp. 503–510.
- Filella, I., Serrano, L., Serra, J., and Peñuelas, J. 1995. Evaluating wheat nitrogen status with canopy reflectance indices and discriminant analysis. *Crop Science*, Vol. 35, pp. 1400–1405.
- Gamon, J.A., Serrano, L., and Surfus, J.S. 1997. The photochemical reflectance index: An optical indicator of photosynthetic radiation-use efficiency across species, functional types, and nutrient levels. *Oecologia*, Vol. 112, pp. 492–501.
- Ganapol, B.D., Johnson, L.F., Hammer, P.D., Hlavka, C.A., and Peterson, D.L. 1998. LEAFMOD: a new within-leaf radiative transfer model. *Remote Sensing of Environment*, Vol. 63, pp. 182–193.
- Gausman, H.W., Allen, W.A., Cardenas, R., and Richardson, A.J. 1970. Relation of light reflectance to histological and physical evaluations of cotton leaf maturity. *Applied Optics*, Vol. 9, pp. 545–552.
- Gitelson, A., and Merzlyak, M.N. 1994. Quantitative estimation of chlorophyll-a using reflectance spectra: experiments with autumn chestnut and maple leaves. *Journal of Photochemistry and Photobiology B: Biology*, Vol. 22, pp. 247–252.
- Gitelson, A.A., and Merzlyak, M.N. 1996. Signature analysis of leaf reflectance spectra: Algorithm development for remote sensing of chlorophyll. *Journal of Plant Physiology*, Vol. 148, pp. 494–500.
- Gitelson, A.A., and Merzlyak, M.N. 1997. Remote estimation of chlorophyll content in higher plant leaves. *International Journal of Remote Sensing*, Vol. 18, pp. 2691–2697.
- Gitelson, A.A., Buschman, C., and Lichtenthaler, H.K. 1999. The chlorophyll fluorescence ratio F735/F700 as an accurate measure of chlorophyll content in plants. *Remote Sensing of Environment*, Vol. 69, pp. 296–302.
- Gitelson, A.A., Gritz, Y.M., and Merzlyak, M.N. 2003. Relationships between leaf chlorophyll content and spectral reflectance and algorithms for non-destructive chlorophyll assessment in higher plant leaves. *Journal of Plant Physiology*, Vol. 160, pp. 271–282.
- Gitelson, A.A., Vina, A., Verma, S.B., Rundquist, D.C., Arkebauer, T.J., Keydan, G., Leavitt, B., Ciganda, V., Burba, G.G., and Suyker, A.E. 2006. Relationship between gross primary production and chlorophyll content in crops: implications for the synoptic monitoring of vegetation productivity. *Journal of Geophysical Research, Atmospheres*, Vol. 111, No. DO8S11.
- Hanrahan, P., and Krueger, W. 1993. Reflection from layered surfaces due to subsurface scattering. In *Proceedings of the 20th Annual Conference on Computer Graphics and Interactive Techniques (SIGGRAPH'93)*, 1–6 August 1993, Anaheim, Calif. ACM Press, New York. pp. 165–174.
- Harron, J.W. 2000. *Optical properties of phytoelements in conifers*. M.Sc. thesis, York University, Toronto, Ont.
- Harron, J.W., and Miller, J.R. 1995. An alternative methodology for reflectance and transmittance measurements of conifer needles. In *Proceedings of the 17th Canadian Symposium on Remote Sensing*, 13–

- 15 June 1995, Saskatoon, Sask. Canadian Aeronautics and Space Institute (CASI), Ottawa, Ont. Vol. 2, pp. 654–661.
- Henye, L.G., and Greenstein, J.L. 1941. Diffuse radiation in the galaxy. *Astrophysics Journal*, Vol. 93, pp. 70–83.
- Horler, D.N.H., Barber, J., and Barringer, A.R. 1980. Effects of heavy metals on the absorbance and reflectance spectra of plants. *International Journal of Remote Sensing*, Vol. 1, pp. 121–136.
- Horler, D.N.H., Dockray, M., and Barber, J. 1983. The red edge of plant leaf reflectance. *International Journal of Remote Sensing*, Vol. 4, No. 2, pp. 273–288.
- Jacquemoud, S., and Baret, F. 1990. PROSPECT: a model of leaf optical properties spectra. *Remote Sensing of Environment*, Vol. 34, pp. 75–91.
- Jacquemoud, S., and Ustin, S.L. 2001. Leaf optical properties: a state of the art. In *Proceedings of the 8th International Symposium on Physical Measurements and Signatures in Remote Sensing*, 8–12 January 2001, Aussois, France. Centre Nationales d'Études Spatiales (CNES), Paris. pp. 223–232.
- Jacquemoud, S., Ustin, S.L., Verdebout, J., Schmuck, G., Andreoli, G., and Hosgood, B. 1996. Estimating leaf biochemistry using the PROSPECT leaf optical properties model. *Remote Sensing of Environment*, Vol. 56, pp. 194–202.
- Kuusik, A. 1998. Monitoring of vegetation parameters on large areas by the inversion of a canopy reflectance model. *International Journal of Remote Sensing*, Vol. 19, pp. 2893–2905.
- le Maire, G., Francois, C., and Dufrene, E. 2004. Towards universal broad leaf chlorophyll indices using PROSPECT simulated database and hyperspectral reflectance measurements. *Remote Sensing of Environment*, Vol. 89, pp. 1–28.
- Moorthy, I., Miller, J.R., and Noland, T.L. 2008. Estimating chlorophyll concentration in conifer needles: an assessment at the needle and canopy level. *Remote Sensing of Environment*, Vol. 112, No. 6, pp. 2824–2838.
- Moran, J.A., Mitchell, A.K., Goodmanson, G., and Stockburger, K.A. 2000. Differentiation among effects of nitrogen fertilization treatments on conifer seedlings by foliar reflectance: a comparison of methods. *Tree Physiology*, Vol. 20, pp. 1113–1120.
- Peñuelas, J., Filella, I., Llusia, J., Siscart, D., and Pinol, J. 1998. Comparative field study of spring and summer leaf gas exchange and photobiology of the mediterranean trees *Quercus ilex* and *Phillyrea latifolia*. *Journal of Experimental Botany*, Vol. 49, pp. 229–238.
- Plonski, W.L. 1974. *Normal yield tables (metric) for major forest species of Ontario*. Division of Forests, Ontario Ministry of Natural Resources, Toronto, Ont. 40 pp.
- Renzullo, L.J., Blanchfield, A.L., Guillermin, R., Powell, K.S., and Held, A.A. 2006. Comparison of PROSPECT and HPLC estimates of leaf chlorophyll contents in a grapevine stress study. *International Journal of Remote Sensing*, Vol. 27, No. 4, pp. 817–823.
- Rock, B.N., Hoshizaki, T., and Miller, J.R. 1988. Comparison of in situ and airborne spectral measurements of the blue shift associated with forest decline. *Remote Sensing of Environment*, Vol. 24, pp. 109–127.
- Slaton, M.R., Hunt, E.R., and Smith, W.K. 2001. Estimating near-infrared leaf reflectance from leaf structural characteristics. *American Journal of Botany*, Vol. 88, pp. 278–284.
- Thomas, S.C. 2005. Increased leaf reflectance in tropical trees under elevated CO₂. *Global Change Biology*, Vol. 11, pp. 197–202.
- Thomas, J.R., and Gausman, H.W. 1977. Leaf reflectance vs. leaf chlorophyll and carotenoid concentrations for eight crops. *Agronomy Journal*, Vol. 69, pp. 799–802.
- Ustin, S.L., Jacquemoud, S., and Govaerts, Y. 2001. Simulation of photo transport in a three-dimensional leaf: implications for photosynthesis. *Plant Cell and Environment*, Vol. 24, No. 10, pp. 1095–1103.
- Vogelmann, T.C. 1993. Plant tissue optics. *Annual Review of Plant Physiology and Plant Molecular Biology*, Vol. 44, pp. 231–251.
- Wang, Z.J., Wang, J.H., Liu, L.Y., Huang, W.J., Zhao, C.J., and Wang, C.Z. 2004. Prediction of grain protein content in winter wheat (*Triticum aestivum* L.) using plant pigment ratio (PPR). *Field Crops Research*, Vol. 90, pp. 311–321.
- Yamada, N., and Fujimura, S. 1988. A mathematical model of reflectance and transmittance of plant leaves as a function of chlorophyll pigment content. In *IGARSS'88, Proceedings of the 8th International Geoscience and Remote Sensing Symposium*, 13–16 September 1988, Edinburgh, Scotland. IEEE, New York. pp. 833–834.
- Zarco-Tejada, P.J., Miller, J.R., Noland, T.L., Mohammed, G.H., and Sampson, P.H. 2001. Scaling-up and model inversion methods with narrowband optical indices for chlorophyll content estimation in closed forest canopies with hyperspectral data. *IEEE Transactions on Geoscience and Remote Sensing*, Vol. 39, No. 7, pp. 1491–1507.
- Zarco-Tejada, P.J., Miller, J.R., Harron, J., Hu, B., Noland, T.L., Goel, N., Mohammed, G.H., and Sampson, P. 2004. Needle chlorophyll content estimation through model inversion using hyperspectral data from boreal conifer forest canopies. *Remote Sensing of Environment*, Vol. 89, pp. 189–199.
- Zarco-Tejada, P.J., Berjón, A., López-Lozano, A.R., Miller, J.R., Martín, P., Cachorro, V., González, M.R., and de Frutos, A. 2005. Assessing vineyard condition with hyperspectral indices: leaf and canopy reflectance simulation in a row-structured discontinuous canopy. *Remote Sensing of Environment*, Vol. 99, No. 3, pp. 271–287.
- Zhang, Y., Chen, J.M., and Thomas, S.C. 2007. Retrieving seasonal variation in chlorophyll content of overstory and understory sugar maple leaves from leaf-level hyperspectral data. *Canadian Journal of Remote Sensing*, Vol. 33, No. 5, pp. 406–415.
- Zhang, Y., Chen, J.M., Miller, J.R., and Noland, T.L. 2008. Leaf chlorophyll content retrieval from airborne hyperspectral remote sensing imagery. *Remote Sensing of Environment*, Vol. 112, No. 7, pp. 3234–3247.